

# Determination of chloride content in cement-based materials; Comparison of results derived by conventional methods and chloride sensor readings

F. Pargar, D.A. Koleva, K. van Breugel

Section of Materials and Environment, Faculty of Civil Engineering and Geosciences, Delft University of Technology, the Netherlands

In this paper the potentiometric response of a Ag/AgCl electrode as a chloride sensor in cementitious materials of different mix design was studied. The chloride sensor's response was discussed with respect to the presence of hydration products around the sensor. The free chloride content inferred from the sensor's response was compared to the one obtained from destructive water and acid soluble chlorides. The measured free chloride content, obtained via sensor's reading, was lower than the obtained water and acid soluble chlorides. The results indicated the influence of the cementitious mix design on the correlation between the free chloride content obtained via sensor's reading, water and acid soluble chlorides.

*Key words: Ag/AgCl sensor, free chloride, cement, chloride binding, water soluble chloride, acid soluble chloride*

## 1 Introduction

The open circuit potential (OCP) response of a Ag/AgCl electrode in any environment can be linked, through the Nernst equation, to the chloride ions activity in this environment. Consequently, a Ag/AgCl electrode can act as a chloride sensor [Elsener et al., 2003; De Vera et al., 2010]. In the case of a cement-based material, as environment, the presence of hydration products around the sensor would affect the sensor's performance. In this regard, the water-to-cement ratio (w/c), type of cement and pore solution composition play an important role. The influence of cement type on the sensor's response has been recently reported [Pargar et al., 2018]. The cement hydration products cover a certain percentage of the surface of the sensor, preventing a direct contact of the sensor's full active surface with the electrolyte. The lower amount of free chloride in these areas is subsequently reflected in the overall sensor's OCP.

A low w/c ratio (e.g. 0.35) results in a dense interfacial zone between cement paste and aggregate, not much different from the density of the bulk cement matrix [Delagrave et al., 1996]. The interfacial zone between aggregate and cement paste with a high w/c ratio (e.g. 0.5) often has a high content of calcium hydroxide and ettringite, elongated C-S-H particles and fewer unhydrated cement particles, compared to that of the bulk matrix [Brandt, 2009]. A high content of ettringite would result in a more porous interfacial zone [Scrivener et al., 2004]. It was shown that portlandite, unlike ettringite, effectively fills up the pores at the interface with aggregate or embedded steel [Bentur and Ish-Shalom, 1974; Page et al., 1981; Zimbelmann, 1985; Maso, 2004; Page, 2009]. A similar trend can be expected at the interface between the sensor and cement paste. The formation of portlandite and ettringite depends on the composition of cementitious materials [van Breugel, 1997; Asbridge et al., 2002]. Consequently, the importance of the cementitious mix design and the cement composition for the sensor's response needs further investigation. This subject has been rarely discussed in the literature so far.

In this paper the influence of water-to-powder ratio (w/p) on the sensor's response is studied. The chloride content inferred from the sensor's response is compared to the one obtained by destructive test methods (acid-soluble and water-soluble chlorides). The observed difference between the chloride contents, determined by the aforementioned methods, is discussed with respect to the chloride binding ability of cement hydration products and the w/p ratio of the mixture. In other words, discussed in this paper are: i) the influence of cementitious mix design and cement composition on the sensor's response; ii) the relation between the chloride content inferred from the sensor's response and the one obtained by destructive test methods.

## 2 Materials and procedures

### 2.1 Specimen preparation and exposure condition

The paste cylinders with cast-in Ag/AgCl sensors were the specimens, subject to investigation in this paper (Figure 1). Mix design and cement compositions of the specimens are presented in Table 1. The chloride sensors were embedded in paste cylinders made of C<sub>3</sub>S with and without addition of C<sub>3</sub>A and gypsum. Different mixtures were employed to study the influence of calcium aluminum sulfate phases, such as ettringite, on the chloride sensor's response. The pure cement phases were supplied by

Mineral Research Processing, France. The cement producer was ENCI cement, The Netherlands.

The sensors were prepared by one-hour anodization of Ag wire in 0.1 M HCl solution at current density of 0.5 mA/cm<sup>2</sup> [Pargar et al., 2018a,b]. The steel wires (1 mm diameter), drawn from low carbon steel, were acetone-cleaned and epoxy-insulated. The sensors and the steel rods were cast-in together in the cylinders in such a manner, that only 1 cm length of both sensor and steel were exposed to the environment (Figures 1a,b), leaving an active surface of 0.39 cm<sup>2</sup> for the steel rods and 0.32 cm<sup>2</sup> for the sensors. The steel rods are not subject to discussion in this work.

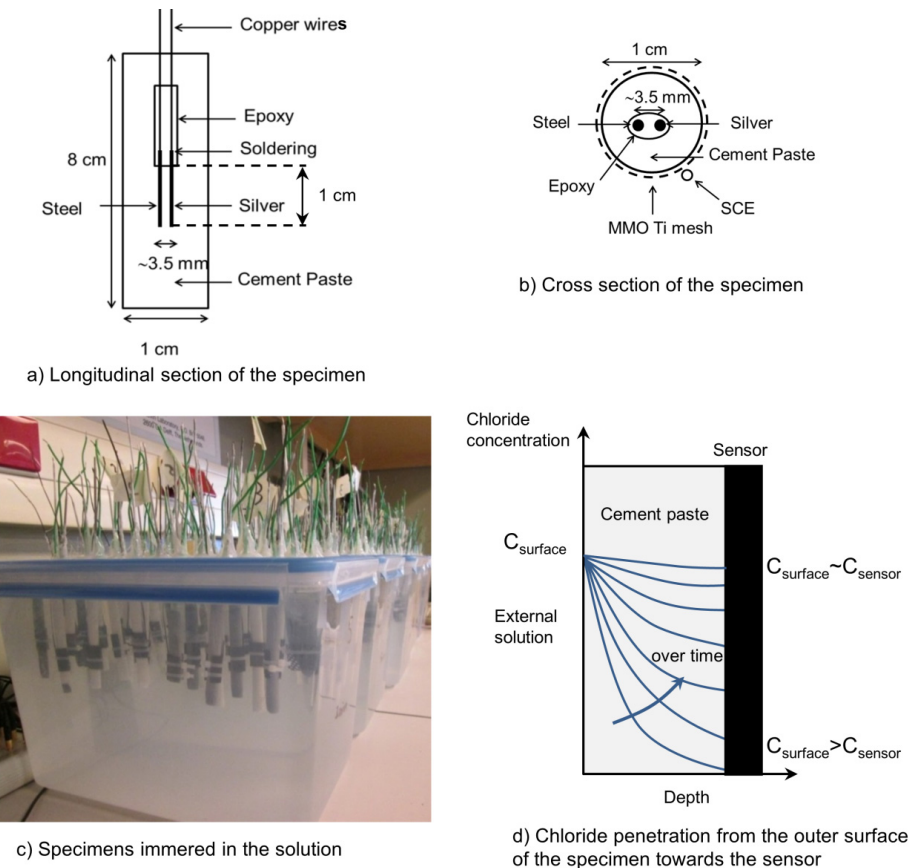


Figure 1: (a) schematic representation of a longitudinal section of the specimen; (b) schematic representation of a cross section of the specimen (designed as 3-electrode type cell); (c) specimens immersed in alkaline solution with different chloride concentration; (d) schematic representation of chloride penetration from external solution towards the sensor's surface

Table 1: Mix designs of the cementitious materials that were used in this study for preparation of the specimens and the chloride content in the solution that specimens were immersed.

w/p ratio	Designated code	C <sub>3</sub> S	C <sub>3</sub> A	Gypsum	Chloride content in the solution (mM)
0.35, 0.4,	C <sub>3</sub> S	100	-	-	0, 10, 100, 500, 1000
0.5	C <sub>3</sub> S+C <sub>3</sub> A	87	10	3	

After curing in a sealed condition for 30 days, the specimens were immersed in a simulated pore solution (0.1 M KOH + Sat. Ca(OH)<sub>2</sub>), pH = 13, with different chloride concentrations (10 mM, 100 mM, 500 mM and 1000 mM). A control case, based on chloride-free solution, was also tested. To keep the concentration of chloride ions as constant as possible, the volume ratio of solution to paste was maintained at 40 [Qiang et al., 2011], and the containers were closed to prevent evaporation (Figure 1c). Two replicates per specimen type were immersed in the solutions. The specimens were retained in the solutions for 300 days to reach a state of equilibrium between the chloride ions in the solution and that in the specimens (Figure 1d).

## 2.2 Test methods

### *Open circuit potential (OCP) measurement*

The cylindrical specimens were immersed in chloride-free and chloride-containing solutions (Table 1, last column). The OCP of the sensors versus saturated calomel electrode (SCE) was monitored during 300 days using PGSTAT 302N potentiostat.

### *Chemical analysis*

The acid-soluble and water-soluble chloride contents in the bulk matrix were determined after 300-day immersion of the specimens in chloride containing solutions (Table 1). The acid-soluble and water-soluble chlorides were extracted from the dried paste samples following the standard procedures [RILEM TC 178-TMC, 2002; RILEM TC 178-TMC, 2002a; ASTM C1152, 2003; ASTM C1218, 2008]. The extracted solutions were analyzed for chloride content with Spectroquant® NOVA 60 photometer and a chloride test set-up (Chloride Cell Test - NO. 114730). The photometer and the chloride test set-up are commercially available from Merck company.

### 3 Results and discussion

#### 3.1 OCP measurement of chloride sensor

##### *Pure cement phases*

The OCP response of the chloride sensor in specimens made of  $C_3S$  with and without addition of  $C_3A$  and gypsum was recorded periodically during 300 days (Figures 2 to 4). Since the sensor's OCP for two replicates per specimen type followed a similar trend, only the average OCP value is presented in these figures. The alteration in the sensor's OCP was evaluated with respect to the w/p ratio, hydration products and the chloride concentration in the medium (10 mM to 1000 mM). The main features of the OCP response of the sensors in  $C_3S$  and  $C_3S+C_3A$  specimens with different w/p ratio (0.35, 0.4, 0.5) are discussed in what follows.

**w/p = 0.35:** The OCP response of the chloride sensors over time was arbitrarily divided into three regions: I, II and III (marked regions in Figures 2 to 4). From the beginning up to day 80 (region I, Figure 2), the OCP of all sensors (except those in the control case "no Cl") sharply dropped towards cathodic values (e.g. Figure 2). From day 80 to day 140 (region II, Figure 2), OCP stabilization of the sensor was observed. The sensor's OCP has reached a more stable potential after 140 days (region III, Figure 2). The time required for the stable sensor's OCP in  $C_3S$  specimens (Figure 2a) is longer than that in  $C_3S+C_3A$  specimens (Figure 2b). This trend was mainly observed in the control case (chloride-free) and in the case of 10 mM chloride concentration (Figure 2a). It can be expected that the sensor in  $C_3S$  specimens was in contact with the pore solution with higher pH than  $C_3S+C_3A$  specimens. The high pH of the pore solution in  $C_3S$  is due to the combined effect of low w/p ratio and the absence of  $C_3A$  and gypsum in the mixture. It is known that the formation of calcium sulfoaluminate in  $C_3S+C_3A$  specimens reduces the alkalinity of the pore solution due to alkali binding by calcium sulfoaluminates [Taylor, 1998; Chappex and Scrivener, 2012]. Therefore, the pH of the pore solution in  $C_3S+C_3A$  specimens would be lower than that in  $C_3S$  specimens. Moreover, the volume of the pore solution in a matrix with high w/p ratio (e.g. 0.5) would be higher than that in a matrix with low w/p ratio (e.g. 0.35). The reduction in the volume of pore solution increases the concentration of soluble alkalis (NaOH and KOH) and the pH of pore solution [Gascoyne, 2002]. As a result, the pH of the pore solution in  $C_3S$  specimens would be highest, due to the synergetic effect of low w/p ratio and less binding of alkalis in this specimen. The pore solution with high pH will lead

to de-chlorination of the AgCl layer. That is why a lower stability of the sensor's OCP in  $C_3S$  specimens was observed after 140 days of immersion in chloride-free and 10 mM chloride-containing solutions (Figure 2a, region III) in comparison to that in  $C_3S+C_3A$  (Figure 2b).

In the chloride-free solution, the sensor's OCP in  $C_3S$  specimen was lower than 140 mV, while the sensor's OCP in  $C_3S+C_3A$  specimen was higher than 150 mV. The more cathodic OCP of the sensor in  $C_3S$  specimen is another evidence for the influence of high pH of the pore solution and de-chlorination of the AgCl layer on the sensor's response.

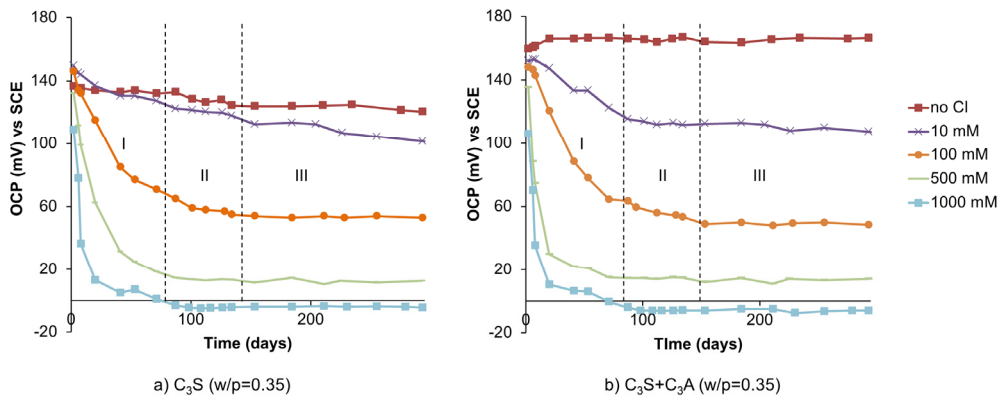


Figure 2: The OCP response of chloride sensor in specimens made of cement components, (a)  $C_3S$  only and (b)  $C_3S$ ,  $C_3A$  and gypsum, with  $w/p = 0.35$  over time

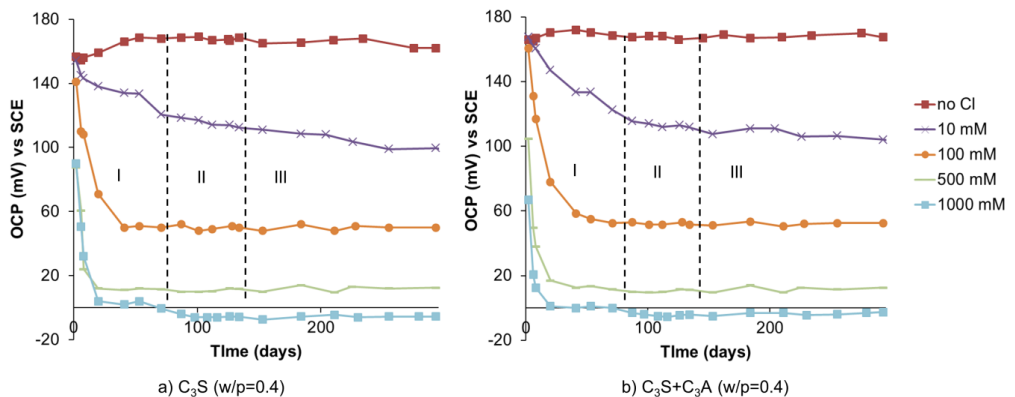


Figure 3: The OCP response of chloride sensor in specimens made of cement components, (a)  $C_3S$  only and (b)  $C_3S$ ,  $C_3A$  and gypsum, with  $w/p = 0.4$  over time

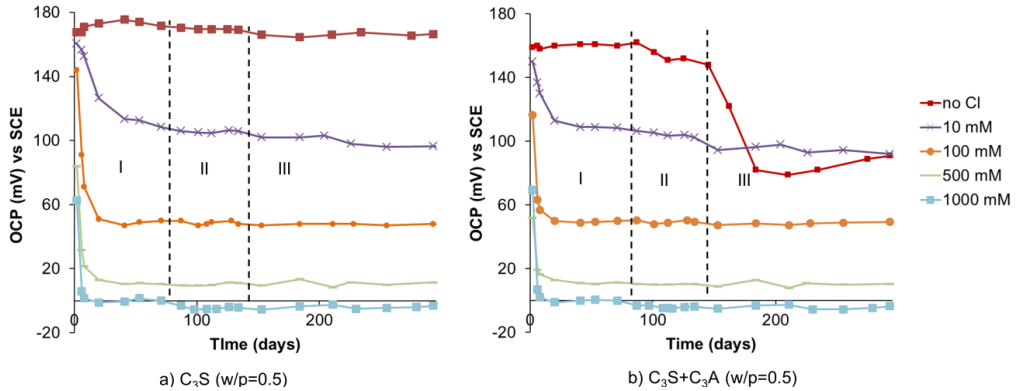


Figure 4: The OCP response of chloride sensor in specimens made of cement components, (a)  $C_3S$  only and (b)  $C_3S$ ,  $C_3A$  and gypsum, with  $w/p = 0.5$  over time

**w/p = 0.4:** The sharp decrease in the sensor's OCP towards cathodic values at the beginning of immersion (region I, Figure 3) is followed by a more stable OCP in the later period (regions II and III, Figure 3).

**w/p = 0.5:** In chloride-containing mediums, the sensor's OCP in specimens with  $w/p = 0.5$  stabilized earlier than the sensor's OCP in specimens with  $w/p = 0.35$  and  $0.4$  (compare Figure 4 with Figures 2 and 3).

In the chloride-free medium (control case), a significant cathodic shift of the sensor's OCP in  $C_3S+C_3A$  specimen after 140 days of immersion (region III, Figure 4) is observed. In this case, the sensor's OCP shifted from around 150 mV (regions I and II, Figure 4b) to values between 70-100 mV (region III, Figure 4b) at which the sensor's OCP was unstable and cannot be described by the Nernst equation for a  $Ag/AgCl$  interface. It was reported that the sensor's OCP in this condition is dependent on adventitious impurities in the medium [de Vera et al., 2010; Suzuki et al., 1998]. This instability of the sensor was not observed in  $C_3S$  ( $w/p = 0.5$ ) - control case (Figure 4a), despite the same  $w/p$  ratio. The instability of the chloride sensor in  $C_3S+C_3A$  ( $w/p = 0.5$ ) is discussed in the following paragraph with respect to the presence of different hydration product at the sensor's surface.

In  $C_3S$  specimens, the reaction of  $C_3S$  with water produces C-S-H and portlandite. In  $C_3S+C_3A$  specimens, the replacement of  $C_3S$  by  $C_3A$  and gypsum (the mix designs were presented in Table 1) generates not only C-S-H and portlandite, but also calcium

sulfoaluminate hydrates with different sulfate content, such as monosulfate and ettringite. In  $C_3S+C_3A$  specimen the ettringite would at least partly replace the portlandite at the sensor's surface (Figure 5a). The portlandite, unlike ettringite, fills up the pores at the paste-sensor interface more effectively (see Figure 5c) [Bentur and Ish-Shalom, 1974; Page et al., 1981; Zimbelmann, 1985; Page, 2009]. Deposition of portlandite at the sensor/paste interface limits the dissolution of silver compounds into the surrounding medium (Figure 5c). In contrast, the presence of ettringite, i.e. a porous hydration product, facilitates de-chlorination of the  $AgCl$  layer, resulting in the presence of metallic silver ( $Ag^0$ ) at the sensor's surface (Figure 5a). The larger amount of  $Ag^0$  subsequently results in an unstable sensor's OCP. Because of this de-chlorination, the lifetime of the sensor embedded in  $C_3S+C_3A$  ( $w/p = 0.5$ ) paste is  $<150$  days (region III, chloride-free in Figure 4) in comparison to that in  $C_3S$  ( $w/p = 0.5$ ) paste. Such a trend was not observed at lower  $w/p$  ratios (0.4 and 0.35). The dense matrix of cementitious material with low  $w/p$  ratio decreases the diffusivity of the matrix and, consequently, the rate of  $AgCl$  de-chlorination. Hence, the lifetime of the sensor in a cement-based matrix with low  $w/p$  ratio (i.e. 0.4, 0.35) is longer. In addition, in pastes with a low  $w/p$  ratio the volume of pore water is also lower, resulting in pore water with higher ionic strength [Flatt and Bowen, 2003]. The activity of chloride ions is lower in a solution with higher ionic strength. The dense matrix of hydration products, together with a reduced chloride ions activity at the sensor's surface, result in a sensor's response different from the one expected for a  $Ag/AgCl$  interface. This is further discussed in the following.

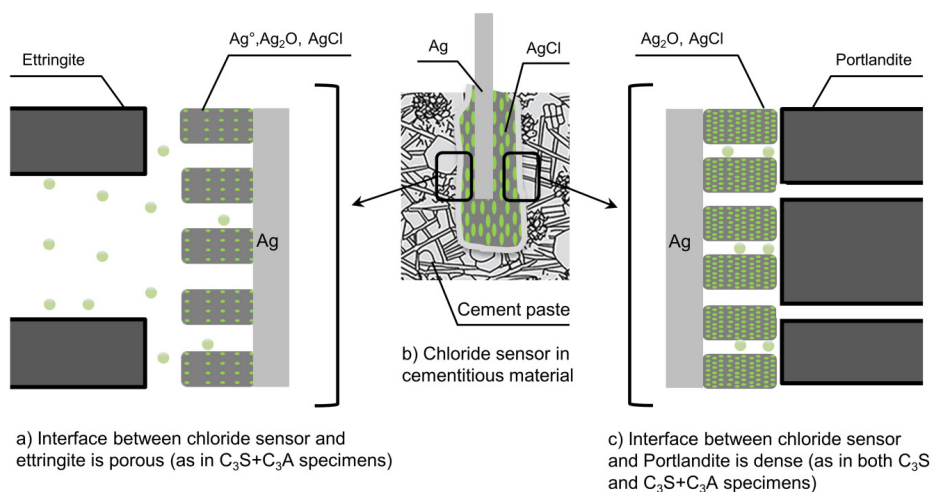


Figure 5: Schematic representation of coverage of the chloride sensor's surface by ettringite (a) and portlandite (c)

*Discussion on the influence of w/p ratio of the pastes on the sensor's OCP*

As discussed above, the presence of cement hydration products around the sensor affects the sensor's OCP response. Figure 6 shows the sensor's OCP after 150-day immersion of specimens in solutions with different chloride content, when most of the sensors

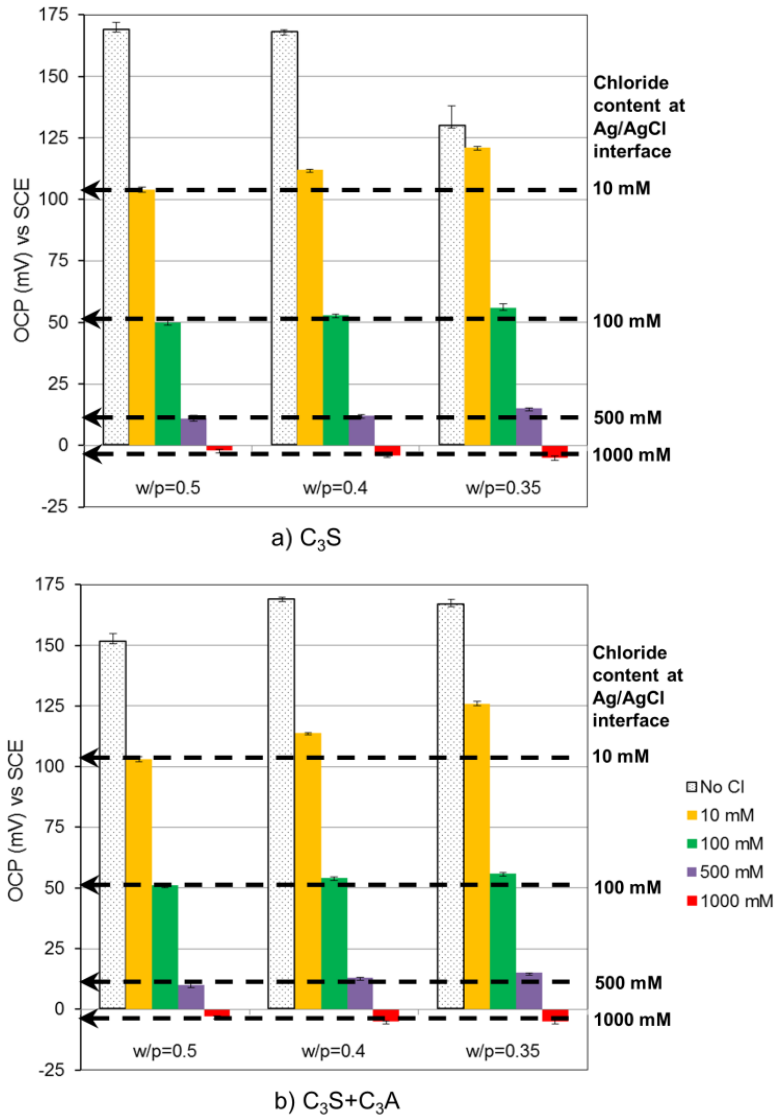


Figure 6: The OCP response of chloride sensor after 150-day immersion of (a) C<sub>3</sub>S specimens and (b) C<sub>3</sub>S+C<sub>3</sub>A specimens in solutions with different chloride concentration. The expected response for a A/AgCl interface at different chloride concentration is specified by dashed line.

demonstrate a stable OCP value. The expected response for a Ag/AgCl interface in chloride-containing solutions [Pargar et al., 2018b] is also presented in Figures 6a,b. The sensor's OCP in chloride-free solution is above 150 mV. The exception is C<sub>3</sub>S (w/p = 0.35) (discussed previously). In the chloride-containing solutions, the sensor's response depends on the w/p ratio of the mixture. Table 2 shows the range of sensor's OCP in C<sub>3</sub>S and C<sub>3</sub>S+C<sub>3</sub>A specimens with different w/p ratio and chloride concentration. It is known that 1 mV difference in the sensor's OCP corresponds to approximately 4% difference in chloride concentration [Angst et al., 2010]. Hence, the OCP difference in Table 2 is also presented as percentage difference in chloride concentration. At 10 mM chloride concentration (Table 2), the embedded sensors in specimens with w/p = 0.35 presented a more anodic OCP (17-23 mV), compared to those in specimens with w/p = 0.5. The more anodic OCP of the sensor in pastes with w/p = 0.35 (C<sub>3</sub>S: 121 mV; C<sub>3</sub>S+C<sub>3</sub>A: 126 mV in Table 2) is an indication for deviation of the sensor's OCP from the expected response for a Ag/AgCl interface (Figures 6a,b). The expected response for a Ag/AgCl interface is 104 mV, which is close to the OCP for specimens with w/p = 0.5 (C<sub>3</sub>S: 104 mV; C<sub>3</sub>S+C<sub>3</sub>A: 103 mV in Table 2). The dense matrix in specimens with w/p = 0.35 together with a lower chloride ions activity at the sensor's surface are the main reasons for the observed deviation. By increasing the chloride concentration to 100 mM and higher, the difference between the sensor's OCP in specimens with w/p ratios of 0.35 and 0.5 decreased to 2-6 mV (Table 2). This OCP difference (2-6 mV) is equivalent to 8-24% difference in chloride concentration (Table 2). This trend demonstrates the lower importance of the w/p ratio for the sensor's response with increasing chloride concentration.

Additionally and in contrast to expectations, at a chloride concentration of 1000 mM the sensor in specimens with w/p = 0.5 was more anodic (2-3 mV, Table 2) than that in specimens with w/p = 0.35. The more anodic OCP of the sensor in specimens with w/p = 0.5 is due to the combined effects of w/p ratio of the mixture and the high chloride concentration (1000 mM). The formation of large crystals of portlandite is pronounced in the mixture with higher w/p ratio (i.e. 0.5) (discussed previously). The dissolution of portlandite increases with increasing the chloride concentration beyond 500 mM [Glasser et al., 1999; Galan and Glasser, 2015]. The lower activity of chloride ions in the pore solution with higher ionic strength (i.e. w/p = 0.5 in 1000 mM chloride concentration) results in a more anodic OCP of the sensor.

Table 2 shows the effect of additions as C<sub>3</sub>A and gypsum on the sensor's response in 10 mM chloride concentration. At 10 mM chloride concentration, the difference between the sensor's OCP in C<sub>3</sub>S specimens with w/p ratios of 0.5 and 0.35 was 17 mV. This difference in C<sub>3</sub>S+C<sub>3</sub>A specimens increased to 23 mV. Hence, addition of C<sub>3</sub>A and gypsum increased the OCP difference from 17 mV to 23 mV. This is due to the presence of different hydration products that builds up a more complex matrix in the C<sub>3</sub>S+C<sub>3</sub>A specimens. Consequently, the influence of w/p ratio on the sensor's OCP is larger in a mixture with a more complex matrix and different hydration products.

Table 2: The range of sensor's OCP for C<sub>3</sub>S and C<sub>3</sub>S+C<sub>3</sub>A specimens with different w/p ratio and chloride concentration. The OCP difference (mV) was also presented as percentage in terms of chloride concentration.

Chloride concentration in external solution (mM)	Sensor's OCP in C <sub>3</sub> S pastes				$\Delta$ OCP mV (%*)	Sensor's OCP in C <sub>3</sub> S+C <sub>3</sub> A pastes				$\Delta$ OCP mV (%*)
	w/p			0.35		w/p			0.35	
	0.5	0.4	0.35			0.5	0.4	0.35		
10	104	112	121	17 (68)	103	114	126	23		
100	50	53	56	6 (24)	51	54	56	5 (20)		
500	11	12	15	4 (16)	10	13	15	5 (20)		
1000	-2	-4	-5	3 (12)	-3	-5	-5	2 (8)		

\* OCP difference in mV multiply by 4 equals to percentage (%) difference in chloride concentration.

### 3.2 Comparison of chloride contents determined by different methods

A schematic presentation of the potential distribution of free chloride, physically bound chloride and chemically bound chloride in cementitious materials is shown in Figure 7. The influence of free and bound chlorides on the chloride content, determined by different methods, is discussed in this section. Three methods for chloride determination were used: (i) leaching in acid (acid-soluble chloride), (ii) leaching in water (water-soluble chloride) and (iii) potentiometry (chloride sensor's response). The acid-soluble chloride is the total (free+bound) chloride content in cementitious materials. The water-soluble chloride is the free chloride plus a part of physically and chemically bound chlorides [RILEM TC 178-TMC, 2002a; Chaussadent and Arliguie, 1999; He et al., 2015]. The sensor can only detect the free chloride content. The distinction of free chloride from water-soluble chloride is difficult [Haque and Kayyali, 1995]. For this reason the measured water-soluble chloride

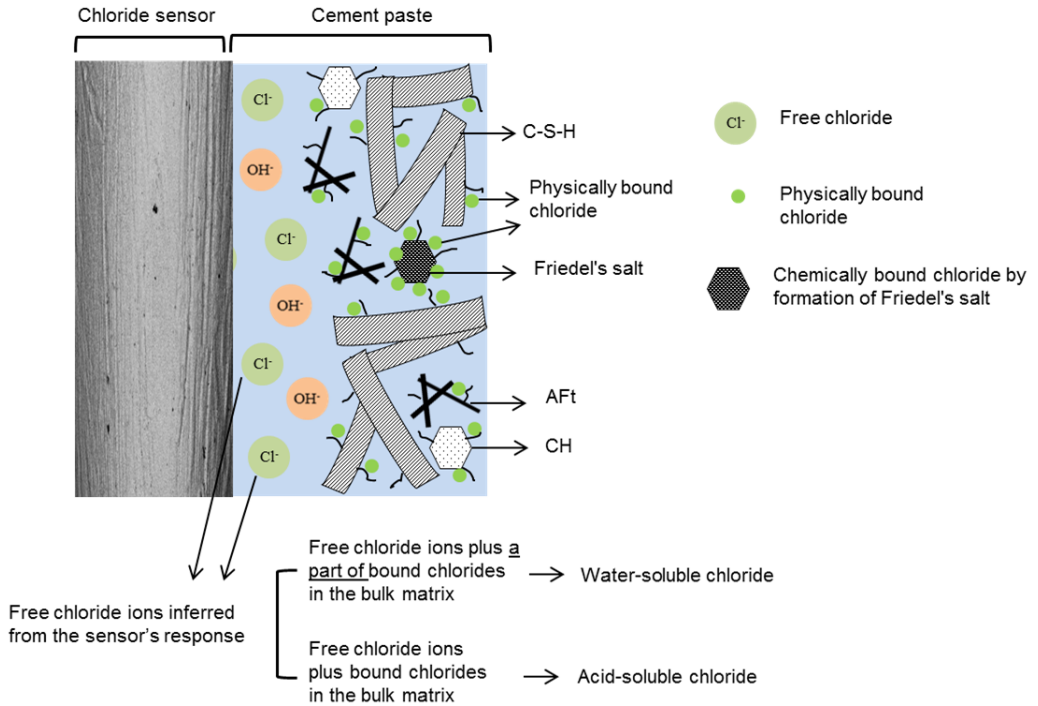


Figure 7: The schematic representation of free chloride ions, chemically bound chloride and physically bound chloride in the cement paste. The sensor's response relies on the free chloride content, while acid-soluble and water-soluble chlorides depend on the amount of bound chlorides in the matrix.

was often considered as the free chloride content [He et al., 2015]. The difference between the water-soluble chloride and the free chloride content inferred from the sensor's response can be significant. This is mainly because the measured water-soluble chloride depends on the amount of bound chlorides released into the water solvent during water-soluble chloride determination. This will be further discussed in this section. The acid-soluble and water-soluble chlorides in the bulk matrix of the specimens are also compared to the free chloride content, inferred from the sensor's response.

#### Acid soluble chloride vs. water soluble chloride

The pastes with various w/p ratio (i.e. 0.35, 0.4, 0.5) (Table 1) were immersed in solutions with different chloride concentration for a period of 300 days. The acid-soluble and water-soluble chloride contents in C<sub>3</sub>S and C<sub>3</sub>S+C<sub>3</sub>A specimens were determined and results are presented in Figure 8.

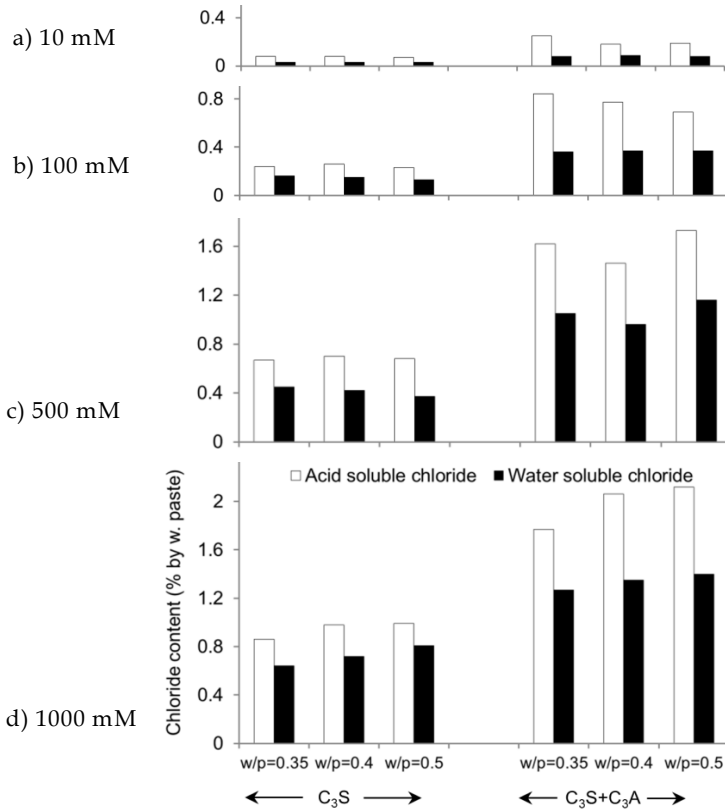


Figure 8: The acid-soluble chloride and water-soluble chloride in C<sub>3</sub>S and C<sub>3</sub>S+C<sub>3</sub>A specimens after 300 days of immersion in solutions with different chloride concentration

In C<sub>3</sub>S specimens chloride ions can only be bound physically. As can be seen in Figure 8, the amount of acid-soluble chloride in C<sub>3</sub>S specimens is higher than the amount of water-soluble chloride. The difference between acid and water-soluble chlorides is, in fact, the portion of physically bound chloride not released into the water solvent during water-soluble chloride determination [Yuan et al., 2011; Hu et al., 2015; He et al., 2016]. The mechanism of physical adsorption of chloride ions to the surface of hydration products was explained in Pargar et al. [2017].

Similar to C<sub>3</sub>S specimens, also in C<sub>3</sub>S+C<sub>3</sub>A specimens the amount of acid-soluble chloride was higher than the amount of water-soluble chloride (Figure 8). The difference between acid and water-soluble chlorides is due to the portion of bound chlorides (chemically and physically) that was not dissolved into the water solvent during the water-soluble chloride

determination. The dissolution of physically bound chloride into the water solvent has a similar explanation as given for  $C_3S$  specimens. The release of chemically bound chloride into the water solvent significantly increased the measured water-soluble chloride [Kopecko and Balazs, 2017]. This is more pronounced in 500 mM and 1000 mM chloride concentrations with higher amount of chemically bound chloride [Pargar et al., 2017].

The acid and water-soluble chlorides in  $C_3S$  specimens were significantly lower than those in  $C_3S+C_3A$  specimens (Figure 8). The  $C_3S$  specimens have no capacity for chemical binding of chloride ions. The chloride ions can be bound chemically in  $C_3S+C_3A$  specimens. The release of chemically bound chloride into the acid and water solvents in  $C_3S+C_3A$  specimens is the main reason for the significantly higher acid and water-soluble chlorides.

#### *Water-soluble chloride vs. sensor reading (sensor's response)*

The free chloride content inferred from the sensor's response (sensor reading), water-soluble chloride and ratio between these two are shown in Figure 9. In this figure, the left vertical axis is the chloride content and the right vertical axis is the calculated ratio. The ratio of one (right vertical axis in Figure 9) indicates that free chloride content (inferred from the sensor's response) is equal to measured water-soluble chloride. The sensor reading of the chloride content was lower than the measured water-soluble chloride in all chloride concentrations. Hence, the ratio of free chloride content to water-soluble chloride was always significantly less than one (Figure 9). This ratio increased from less than 0.2 in a 10 mM chloride concentration to 0.8 in 500 mM and 1000 mM chloride concentrations. The maximum ratio ( $>0.8$ ) was observed in  $C_3S$  ( $w/p = 0.5$ ) specimens, with only physically bound chlorides, in 500 mM and 1000 mM chloride concentrations. In other words, the ratio was closer to one when cementitious materials with high  $w/p$  ratio (e.g. 0.5) and only physical chloride binding ability (e.g.  $C_3S$  specimens), were in high chloride concentration (e.g. 500 mM and 1000 mM). These results show that paste composition and  $w/p$  ratio, on the one hand, and chloride concentration in the medium, on the other hand, affect the correlation between the free chloride and the water-soluble chloride.

The difference between the water-soluble chloride and the sensor reading of the chloride content in  $C_3S$  specimens is lower than that difference in  $C_3S+C_3A$  specimens (Figure 9). As previously mentioned, the release of bound chlorides into the water solvent plays a significant role in the measured water-soluble chloride. The release of bound chlorides into

the water solvent is larger in  $C_3S+C_3A$  specimens (due to the chemical chloride binding ability) than that in  $C_3S$  specimens. This results in a larger difference between the water-soluble chloride and the sensor reading of the chloride content in  $C_3S+C_3A$  specimens than that in  $C_3S$  specimens.

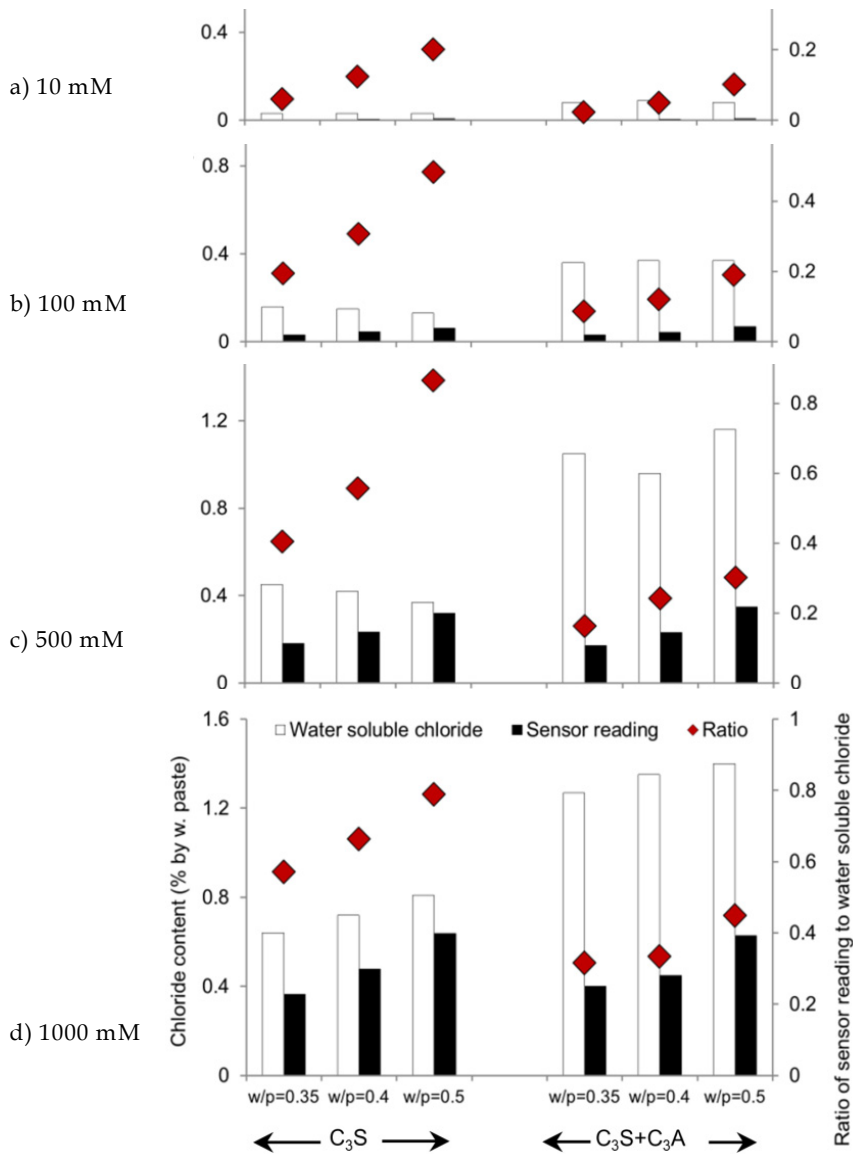


Figure 9: The water-soluble chloride, sensor reading of the free chloride content and the ratio of sensor reading to water-soluble chloride for  $C_3S$  and  $C_3S+C_3A$  specimens after 300 days of immersion in solutions with different chloride concentration

Water-soluble chloride is often considered to be equal to the free chloride content [He et al., 2015]. After 300-day immersion of the specimens in chloride containing solutions, the free chloride content in the pore water of  $C_3S$  and  $C_3S+C_3A$  specimens would be close to each other [Arya et al., 1987]. In Figure 9, the change in the sensor reading of the chloride content is significantly lower than the change in the measured water-soluble chloride. As mentioned in the previous paragraph, the release of bound chlorides into the water solvent plays a significant role in the measured water-soluble chloride. Consequently, sensor reading of the chloride content is more accurate than water-soluble chloride for determination of the free chloride content in cementitious materials.

#### *Relation between free and bound chlorides*

Figure 10 shows the share of free and bound chlorides in the total chloride content in  $C_3S$  and  $C_3S+C_3A$  specimens. This figure represents the acid-soluble, water-soluble and free chloride contents (inferred from the sensor's response) in the specimens at different chloride concentration. As previously shown, the measured chloride contents determined with different methods were in the following order: acid-soluble chloride > water-soluble chloride > free chloride. In Figure 10 the acid-soluble chloride (total chloride) was set as 100%. Then the water-soluble chloride and the free chloride (inferred from the sensor's response) were normalized against the total chloride.

The chloride in  $C_3S$  specimens was present as free and physically bound chlorides (Figure 10a). The free chloride in Figure 10a is the ratio of sensor reading of the chloride content to total chloride content. The subtraction of the free chloride content from the total chloride yields the physically bound chloride (Figure 10a). The difference between the water-soluble chloride and free chloride was also attributed to the physically bound chloride (Figure 10a). The free chloride content increased from about 10% in a 10 mM chloride concentration to 60% in a 1000 mM chloride concentration. The larger free chloride content in higher chloride concentration is the result of a decrease in the physical chloride binding capacity of the hydration products.

The chloride in  $C_3S+C_3A$  specimens was present as free chloride, physically bound chloride and chemically bound chloride (Figure 10b). Similar to what has been said about the chloride in the  $C_3S$  pastes, the free chloride in Figure 10b was determined from the ratio of sensor reading of the chloride content to total chloride content. However, the borderline between chemically bound chloride and physically bound chloride was

assumed. As discussed previously, the release of chemically bound chloride into the water solvent is significantly higher than the release of physically bound chloride (Figure 10b). Hence, the difference between the measured water-soluble chloride and the free chloride was attributed to the chemically bound chloride (Figure 10b). For the same reason (i.e. significant release of chemically bound chloride into the water solvent), the difference between the acid and water-soluble chlorides in Figure 10b was attributed to the physically bound chloride.

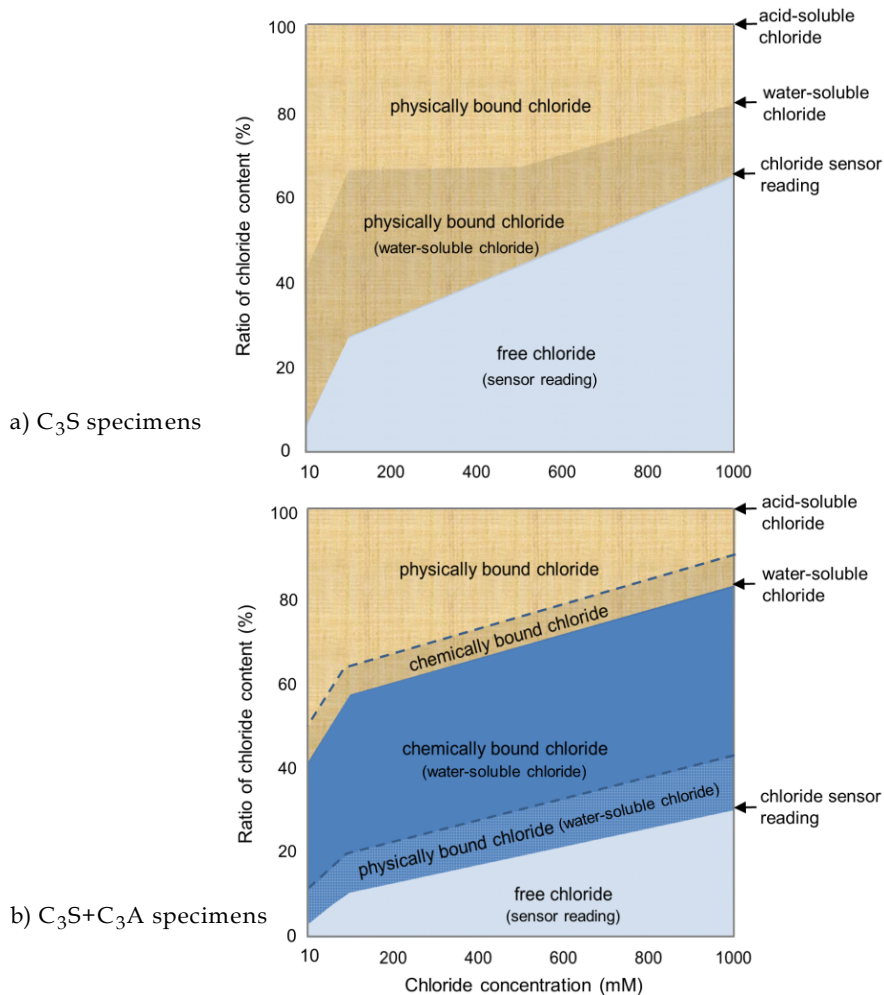


Figure 10: The contribution of free chloride, physically bound chloride and chemically bound chloride to the total chloride content in the cementitious materials. The free chloride was measured by chloride sensor.

In the presence of chemically bound chloride, as in the  $C_3S+C_3A$  specimen, the free chloride content significantly decreased to about 5% and 30% in 10 mM and 1000 mM chloride concentrations, respectively (Figure 10b). In other words, for the same free chloride concentration, the percentage of bound chloride in  $C_3S+C_3A$  specimens was higher than that in  $C_3S$  specimens (as expected). This is due to the significant contribution of the chemically bound chloride to the total bound chloride in  $C_3S+C_3A$  specimens. The water-soluble chloride and the free chloride contents in  $C_3S$  specimens were closer to each other, compared to those in  $C_3S+C_3A$  specimens (compare Figures 10a with 10b). This is as expected, since the  $C_3S$  has no ability for chemical binding of chloride ions. The chemically bound chloride is responsible for the large difference between the water-soluble chloride and the free chloride content in  $C_3S+C_3A$  specimens (Figure 10b).

The results presented in this paper show that the stability of a Ag/AgCl chloride sensor in cementitious materials is the major challenge for its application. A stable sensor's response depends on the concentrations of chloride and hydroxide ions in the paste. The deposition of hydration products on the sensor's surface influences the stable OCP of the sensor. The extent of this influence depends on the w/p ratio of the paste. The high alkalinity of the pore water in a low w/p ratio (0.35) significantly affects the stable sensor's OCP, especially at low chloride concentration (e.g. 10 mM). The higher accessibility of pore water to the sensor in the mixture with high w/p ratio (0.5) can result in de-chlorination of the AgCl layer and unstable sensor's OCP in chloride-free cementitious materials.

In summary, the free chloride determination in cementitious materials needs knowledge of the surrounding medium. The environment in a  $C_3S$  paste is different from that in a  $C_3S+C_3A$  paste. In addition to the concerns for lifetime and stability of the chloride sensor in cementitious materials, the application of the potentiometry method is a feasible and reliable approach for a continuous and non-destructive determination of the chloride content.

## 4 Conclusions

In this paper, the performance of a Ag/AgCl sensor in cementitious materials with different mix design and cement composition was evaluated. Based on the obtained results the following conclusions can be drawn:

- The sensor's OCP in a cement-based matrix with low chloride concentration (e.g. 10 mM) depends on the w/p ratio of the mixture. The sensor's OCP in specimens with low w/p ratio (0.35) is more anodic than the expected response for a Ag/AgCl interface (as observed in specimens with high w/p ratio (0.5)). The more anodic sensor's OCP in specimens with w/p = 0.35 indicates the lower accuracy in determination of the free chloride content in mixtures with low w/p ratio. This is the result of a dense matrix of cement hydration products, higher ionic strength and lower activity of chloride ions on the sensor's surface. By increasing the chloride concentration to 100 mM and higher, the dependency of the sensor's OCP on the cementitious mix design decreases.
- The free chloride content inferred from the sensor's response (sensor reading) is lower than the measured water and acid soluble chlorides. The free and water-soluble chloride contents are closer to each other in C<sub>3</sub>S specimens than those in C<sub>3</sub>S+C<sub>3</sub>A specimens. This trend is pronounced at higher chloride concentration (e.g. 1000 mM). This observation indicates the importance of cement composition, w/p ratio and chloride concentration in the cement-based matrix for the correlation between the free, water-soluble and acid-soluble chlorides.
- On the one hand, a decrease in w/p ratio lowers the content of pore water around the sensor and the rate of AgCl dissolution. This subsequently reduces the reliability of the sensor for determination of chloride ions concentration in the environment. On the other hand, an increase in w/p ratio results in a higher amount of pore water around the sensor. A higher percentage of the sensor's surface can be in direct contact with the pore water. Hence, the sensor can reflect the chloride content in the pore water in a shorter period.

## Literature

- Angst U. and Polder R. (2014). Spatial variability of chloride in concrete within homogeneously exposed areas, *Cement and Concrete Research*, Vol. 56, p. 40-51.
- Angst, U., Elsener, B., Larsen, C. K. and Vennesland, O. (2010). Potentiometric determination of the chloride ion activity in cement-based materials, *Journal of Applied Electrochemistry*, Vol. 40(3), p. 561-573.
- Arya, C., Buenfeld, N. R. and Newman, J. B. (1987). Assessment of simple methods of determining the free chloride ion content of cement paste, *Cement and Concrete Research*, Vol. 17(6), p. 907-918.
- Asbridge, A. H., Page, C. L. and Page, M. M. (2002). Effects of metakaolin, water/binder ratio and interfacial transition zones on the microhardness of cement mortars, *Cement and Concrete Research*, Vol. 32(9), p. 1365-1369.
- ASTM C1152. (2003). *Standard Test Method for Acid-Soluble Chloride in Mortar and Concrete*, American Society for Testing and Materials (ASTM) Philadelphia, PA.
- ASTM C1218. (2008). *Standard Test Method for Water-Soluble Chloride in Mortar and Concrete*, American Society for Testing and Materials (ASTM) Philadelphia, PA.
- Bentur, A. and Ish-Shalom, M. (1974). Properties of type K expansive cement of pure components II. Proposed mechanism of ettringite formation and expansion in unrestrained paste of pure expansive component, *Cement and Concrete Research*, Vol. 4(5), p. 709-721.
- Brandt, A.M. (2009). *Cement-Based Composites: Materials, Mechanical Properties and Performance*, Taylor & Francis.
- Chappex, T. and Scrivener, K. (2012). Alkali fixation of C-S-H in blended cement pastes and its relation to alkali-silica reaction, *Cement and Concrete Research*, Vol. 42(8), p. 1049-1054.
- Chaussadent, T. and Arliguie, G. (1999). AFREM test procedures concerning chlorides in concrete: extraction and titration methods, *Materials and Structures*, Vol. 32, p. 230-234.
- Cwirzen, A. and Penttala, V. (2005). Aggregate-cement paste transition zone properties affecting the salt-frost damage of high-performance concretes, *Cement and Concrete Research*, Vol. 35(4), p. 671-679.
- De Vera, G., Climent, M. A., Antón, C., Hidalgo, A., & Andrade, C. (2010). Determination of the selectivity coefficient of a chloride ion selective electrode in alkaline media simulating the cement paste pore solution, *Journal of Electroanalytical Chemistry*, Vol. 639(1), p. 43-49.

- Delagrave, A., Pigeon, M., Marchand, J. and Revertegeat, E. (1996). Influence of Chloride ions and pH level on the durability of high-performance cement pastes (Part II), *Cement and Concrete Research*, Vol. 26(5), p. 749-760.
- Elsener, B., Zimmermann, L. and Bohni, H. (2003). Non-destructive determination of the free chloride content in cement-based materials, *Materials and Corrosion*, Vol. 54 (6), p. 440-446.
- Evans, D. G. and Duan, X. (2006), *layered double hydroxides, Structure and Bonding*, Springer book, Vol. 119 (2006), p. 1-87.
- Femenias, Y. S., Angst, U., Caruso, F. and Elsener, B. (2016). Ag/AgCl ion-selective electrodes in neutral and alkaline environments containing interfering ions, *Materials and Structures*, Vol. 49(7), p. 2637-2651.
- Flatt, R. J. and Bowen, P. (2003). Electrostatic repulsion between particles in cement suspensions: Domain of validity of linearized Poisson-Boltzmann equation for nonideal electrolytes, *Cement and Concrete Research*, Vol. 33(6), p. 781-791.
- Galan, I. and Glasser, F. P. (2015). Chloride in cement, *Advances in Cement Research*, Vol. 27(2), p. 63-97.
- Gascoyne, M. (2002). *Influence of grout and cement on groundwater composition*, Possiva, Working Report, 7.
- Glasser, F., Tyrer, M. and Quillin, K. (1999). *The chemistry of blended cements and backfills intended for use in radioactive waste disposal*, (No. EA-RD-TR-P--98). Environment Agency.
- Graedel, T. E. (1992). Corrosion mechanisms for silver exposed to the atmosphere, *Journal of the Electrochemical Society*, Vol. 139(7), p. 1963-1970.
- Haque, M. N. and Kayyali, O. A. (1995). Free and water-soluble chloride in concrete, *Cement and Concrete Research*, Vol. 25(3), p. 531-542.
- He, F., Shi, C., Chen, C. and An, X. (2015). Relationship between water-soluble and free chloride concentrations in cement-based materials, *Materials Research Innovations*, Vol. 19(sup8), S8-348.
- He, F., Shi, C., Hu, X., Wang, R., Shi, Z., Li, Q. and An, X. (2016). Calculation of chloride ion concentration in expressed pore solution of cement-based materials exposed to a chloride salt solution, *Cement and Concrete Research*, Vol. 89, p. 168-176.
- Hewlett, P. C. (2003). *Lea's chemistry of cement and concrete (Fourth Edition)*, Butterworth-Heinemann, Elsevier Ltd.
- Hu, X., Shi, C. and De Schutter, G. (2015). Influences of chloride immersion on zeta potential and chloride in concentration of cement-based materials, *14th International Congress on the Chemistry of Cement*, p. 1-15.

- Kopecko, K. and Balazs, G. L. (2017). Concrete with improved chloride binding and chloride resistivity by blended cement, *Advances in Materials Science and Engineering*, 2017-7940247.
- Levard, C., Hotze, E. M., Lowry, G. V. and Brown Jr, G. E. (2012). Environmental transformations of silver nanoparticles: impact on stability and toxicity, *Environmental Science and Technology*, Vol. 46(13), p. 6900-6914.
- Mangat, P. S. and Molloy, B. T. (1995). Chloride binding in concrete containing PFA, GBS or silica fume under sea-water exposure, *Magazine of Concrete Research*, Vol. 47(171), p. 129-141.
- Maso, J. C. (2004). *Interfaces in cementitious composites*. CRC Press.
- Matschei, T., Lothenbach, B. and Glasser, F. (2007). Thermodynamic properties of Portland cement hydrates in the system  $\text{CaO-Al}_2\text{O}_3\text{-SiO}_2\text{-CaSO}_4\text{-CaCO}_3\text{-H}_2\text{O}$ , *Cement and Concrete Research*, Vol. 37(10), p. 1379-1410.
- NEN-EN 197-1 (2011). *Cement - Part 1: Composition, specifications and conformity criteria for common cements*, European Committee for Standardization.
- Page, C. L. (2009). Initiation of chloride-induced corrosion of steel in concrete: role of the interfacial zone, *Materials and corrosion*, Vol. 60(8), p. 586-592.
- Page, C. L., Short, N. R. and El Tarras, A. (1981). Diffusion of chloride ions in hardened cement pastes, *Cement and Concrete Research*, Vol. 11(3), p. 395-406.
- Pargar, F., Koleva, D. A. and van Breugel, K. (2017). Determination of chloride content in cementitious materials: from fundamental aspects to application of Ag/AgCl chloride sensors. *Sensors*, 17(11), 2482.
- Pargar, F., Koleva, D. A. and van Breugel, K. (2018). Potentiometric response of Ag/AgCl sensor in Portland and slag cement pastes, *Proceeding of the Workshop on Concrete Modelling and Materials Behaviour in Honor of Professor Klaas van Breugel*, RILEM Publications, Delft, The Netherlands, p. 214-221.
- Pargar, F., Kolev, H., Koleva, D. A. and van Breugel, K. (2018a). Microstructure, surface chemistry and electrochemical response of Ag/AgCl sensors in alkaline media. *Journal of Materials Science*, Vol. 53(10), p. 7527-7550.
- Pargar, F., Kolev, H., Koleva, D. A. and van Breugel, K. (2018b). Potentiometric Response of Ag/AgCl Chloride Sensors in Model Alkaline Medium. *Advances in Materials Science and Engineering*, 2018.
- Payer, J. H., Ball, G., Rickett, B. I. and Kim, H. S. (1995). Role of transport properties in corrosion product growth, *Materials Science and Engineering: A*, Vol. 198(1-2), p. 91-102.

- Qiang, Y., Caijun, S., De Schutter, G., Dehua, D. and Fuqiang, H. (2011). Chloride ion concentration on the surface of cement-based materials in chloride solutions, *Journal of the Chinese ceramic society*, Vol. 39(3), p. 544-549.
- Rajbhandari, A., Yadav, A. P., Manandhar, K. and Pradhananga, R. R. (2009). Characterization and applications of silver sulphide based membrane electrodes, *Scientific World*, Vol. 7(7), p. 19-23.
- Raynauld, J. P. and Laviolette, J. R. (1987). The silver-silver chloride electrode: a possible generator of offset voltages and currents, *Journal of neuroscience methods*, Vol. 19(3), p. 249-255.
- RILEM TC 178-TMC. (2002). Analysis of total chloride in concrete, *Material and Structures*, 35, p. 583-585.
- RILEM TC 178-TMC. (2002a). Analysis of water-soluble chloride content in concrete, Recommendation, *Materials and Structures*, Vol. 35, p. 586-588.
- Scrivener, K. L., Crumbie, A. K. and Laugesen, P. (2004). The interfacial transition zone (ITZ) between cement paste and aggregate in concrete, *Interface Science*, Vol. 12(4), p. 411-421.
- Suzuki, H., Hiratsuka, A., Sasaki, S. and Karube, I. (1998). Problems associated with the thin-film Ag/AgCl reference electrode and a novel structure with improved durability, *Sensors and Actuators B: Chemical*, Vol. 46(2), p. 104-113.
- Taylor, H. F. W. (1998). *Cement Chemistry*, 2nd Edit, Thomas Telford Publication.
- van Breugel, K. (1991). *Simulation of hydration and formation of structure in hardening cement-based materials*, Ph.D. Thesis, Delft University of Technology, The Netherlands.
- Yang, Z., Fischer, H. and Polder, R. (2013). Modified hydrotalcites as a new emerging class of smart additive of reinforced concrete for anticorrosion applications: a literature review, *Materials Corrosion*, Vol.64(12), p. 1066-1074.
- Yoon, S., Moon, J., Bae, S., Duan, X., Giannelis, E. and Monteiro, P. (2014). Chloride adsorption by calcined layered double hydroxides in hardened Portland cement paste, *Materials Chemistry and Physics*, Vol. 145(3), p. 376-386.
- Yuan, Q., Deng, D., Shi, C. and De Schutter, G. (2013). Chloride binding isotherm from migration and diffusion tests, *Journal of Wuhan University of Technology-Mater. Sci. Ed.*, Vol. 28(3), p. 548-556.
- Yuan, Q., Deng, D., Shi, C. and De Schutter, G., Deng, D. and He, F. (2011). Chloride-ion concentration on the surface of cement-based materials in chloride solutions, *Journal of the Chinese ceramic society*, Vol. 39(3), p. 544-549.

Zimbelmann, R. (1985). A contribution to the problem of cement-aggregate bond, *Cement and Concrete Research*, Vol. 15(5), p. 801-808.